CME SHOCK COLLISIONS AND MAGNETIC CLOUD IMPACT

S. Poedts[1], B. Van der Holst[1], H. De Sterck[1], L. Van Driel-Gesztelyi[1], Á. Csík[2], A. Milesi[2], and H. Deconinck[2]

[1]Centre for Plasma Astrophysics, K.U.Leuven, Celestijnenlaan 200B, 3001 Leuven, Belgium
[2]Von Karman Institute, Waterloose steenweg 721, 1640 Sint-Genesius-Rode, Belgium

ABSTRACT

The shocks in the solar corona caused by fast Coronal Mass Ejections (CMEs) and the shock transitions at the Earth's magnetosphere caused by the impact of the corresponding magnetic clouds (superposed on the solar wind) are studied in the framework of computational magnetohydrodynamics (MHD). Due to the presence of three characteristic velocities and the anisotropy induced by the magnetic field, MHD shocks can have a complicated structure including secondary shock fronts, overcompressive and compound shocks, etc. Numerical simulations show that CME shocks (in the lower corona) and the shock at the Earth's magnetosphere (at times of the impact of a magnetic cloud) have such a complex structure.

Simulations of MHD shock collisions are presented and discussed. Such complex events involving two or more CMEs are actually observed and the complexity may allow to derive some parameters from the observations. In addition, time dependent simulations show how the magnetic reconnection at the Earth's bow shock is affected by the magnetic cloud impact. The CME shocks are important for 'space weather' because they can easily be observed in radio wavelengths. This makes it possible to track the position of the CMEs/magnetic clouds and, hence, to follow their propagation through the corona and IP space. The topology of the shock at the Earth's magnetosphere at the impact of a magnetic cloud is important for the 'geo-effectiveness' of the magnetic storms. Hence, the *complex* MHD shocks and shock interactions play a *key* role in both observations and theory of space weather!

Key words: CMEs, magnetic clouds, MHD shocks, numerical simulations.

1. MOTIVATION AND MODELING (SUB-)PROBLEMS

The term 'Space weather' refers to the conditions in space (the Sun, the solar wind as well as the Earth's upper atmosphere) that affect Earth and its technological systems and can even endanger human life or health. Many organizations (e.g. NASA, ESA, and others) spend a lot of effort to provide and improve predictions of space weather events in the hope to be able take protective measures against predicted magnetic storms. More reliable predictions, however, require a better insight in the physical processes on the Sun and in the solar wind that drive and affect the space weather events. However, these physical processes are a very complicated mixture of solar events, solar energetic particle injections, cosmic rays, magnetospheric, ionospheric, and thermospheric perturbations, etc, and occur on a wide range of time and length scales. As a consequence, the theoretical modeling of the *key problem*, viz. to understand the 'physics' of Space Weather, requires a joint, multi-disciplinary approach. CMEs and the MHD shocks they give rise to play a *crucial role* in space weather and a careful study of these violent and complex phenomena is essential for a deeper insight in space weather physics.

In the present paper, is is claimed that the *CME related MHD shocks play a* **key role** *in several space weather (sub-)problems*. E.g. in the sub-problem regarding why and how CMEs are initiated, the MHD shocks caused by fast CMEs can have a complex structure composed of different types of MHD shocks (De Sterck and Poedts (1999a,b,c)). Below it will be argued that precisely this complexity combined with the fact that these shocks are visible in radio wavelengths, may contain clues for determining CME initiation parameter values. Next, there is the sub-problem of the observation and modeling of the propagation of CMEs and, in particular, the evolution of the CME structure and the leading shock fronts during their propagation through the interplanetary medium needs to be studied. About two thirds of the interplanetary (IP) ejecta turns out to be complex, i.e. lasting several days and consisting of two or more CMEs coming together and interacting. Detailed comparison of radio observations and theoretical models for such interacting shock fronts may reveal information on the respective speeds, shock strengths, etc., and is absolutely necessary for predictions of arrival times of IP ejecta at Earth. Last but not least, the impact of the CMEs or magnetic clouds on the Earth's magnetosphere is another important subproblem in which the MHD shock complexity is important. In particular, the interaction of the CME leading shock front with the bow shock at the Earth's magnetosphere drastically affects the reconnection characteristics of the magnetic field lines and, hence, certainly influences the 'geo-effectiveness' of the magnetic storms.

The CME related complex MHD shocks are claimed to play a **key role** in the above-mentioned sub-problems concerning CME initiation, propagation, and the interaction of magnetic clouds with the bow shock at the Earth's magnetosphere. Below, we will first discuss the possible components of complex MHD shocks generated by fast CMEs, since it is precisely this complexity that enables to distinguish between different parameter domains. Next, we discuss new 2D simulation results on the interaction of such MHD shocks with different speeds during their propagation between the Sun and the Earth. We then present new results of 3D time-dependent simulations of the interaction of a magnetic cloud with the bow shock at the Earth's magnetosphere. This clearly demonstrates the dramatic consequences such magnetic cloud impacts can have on the structure of the magnetospheric bow shock. The possible consequences for the 'geo-effectiveness' of the related magnetic storms is discussed and a challenging hypothesis on this issue is formulated.

2. MHD SHOCK TYPES: THE BUILDING BLOCKS

As is well-known from fluid dynamics, an object placed in a supersonic flow causes the flow to create a parabolic bow shock in front of the object in order to get around it. The same happens in a magnetized plasma flow. In a magnetized plasma, however, the magnetic field introduces a preferred direction and thus *anisotropy*. In addition, in the (macroscopic) MHD description of such a plasma, there exist *three basic MHD wave modes*, viz. the Alfvén wave and the slow and fast magnetosonic waves, instead of only sound waves. As a result, MHD shocks can be much more complex than the shocks in hydrodynamic systems which have only one (isotropic) wave speed. The characteristic velocities corresponding to the three MHD waves depend on the direction of propagation. For a direction labeled by x, these velocities are denoted by c_{Ax}, c_{sx}, and c_{fx}, respectively. For any direction x they satisfy the relation

$$c_{fx} \geq c_{Ax} \geq c_{sx}.$$

Suppose now that the $x-$direction denotes the direction perpendicular to the shock front. The above inequalities then yield four possible positions for the normal plasma speed, v_x, viz.

$$[1] \geq c_{fx} \geq [2] \geq c_{Ax} \geq [3] \geq c_{sx} \geq [4].$$

This corresponds to four plasma states satisfying given values for the fluxes of mass, momentum, magnetic field and energy. Each pair of those four states satisfies the Rankine-Hugoniot 'jump' conditions and can thus be connected by a shock. Consequently, there exist three types of MHD shocks called 1) **fast shocks**, in which the flow speed drops from super-fast to sub-fast but super-Alfvénic, i.e. from position [1] to [2], in the shock; 2) **slow shocks**, in which the flow speed drops from sub-Alfvénic but super-slow to sub-slow, i.e. from position [3] to [4], in the shock; and 3) **intermediate shocks**, in which the flow speed drops from super-Alfvénic to sub-Alfvénic, i.e. from [1] to [3], from [1] to [4], from [2] to [3], or from [2] to [4]. Some of the properties of these shocks are summarized in Fig. 1 (a–c).

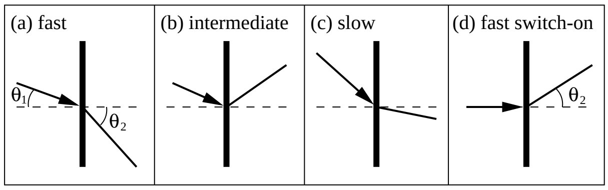

Figure 1. Some properties of basic MHD shocks. The thick vertical line denotes the shock front, the dashed line is the shock normal. The arrowed lines denote magnetic field lines that are refracted through the shock surface. The region left from the shock front is upstream, right is downstream. (From De Sterck (1999)).

In fast shocks ([1]–[2]) the tangential component of the magnetic field is increased so that the magnetic field lines are refracted away from the shock normal (i.e. $\theta_2 > \theta_1$ in Fig. 1a). In slow shocks ([3]–[4]), on the other hand, the magnetic field lines are refracted towards the shock normal (see Fig. 1c); while intermediate shocks change the sign of the tangential component of the magnetic field (see Fig. 1b).

Each of the MHD shock types has a 'limiting case'. A fast 'switch-on' shock, e.g., has a vanishing tangential component of the magnetic field upstream, but a finite one downstream, as indicated in Fig. 1d. Similarly, in a slow 'switch-off' shock this magnetic field component is 'switched off' by the shock, i.e. it vanishes downstream. A [1]–[4] 'hydrodynamic' shock is a limiting case of an intermediate shock that does not change the magnetic field which is perpendicular to the shock front in that case.

Intermediate shocks and 'fast switch-on' shocks can only occur for some well-specified regime of the upstream parameters (Kennel et al (1989); Steinolfson and Hundhausen (1990)). Switch-on shocks are intrinsically magnetic phenomena that have no analogue in hydrodynamic flows of neutral fluids. They can only occur when the upstream magnetic field, B_1, is 'dominant'. The flow speed has to satisfy two conditions which, in terms of the upstream magnetic field read:

$$B_1^2 > \gamma p_1, \tag{1}$$

and

$$B_1^2 > \rho_1 v_{x,1}^2 \, \frac{\gamma - 1}{\gamma(1-\beta_1)+1}, \tag{2}$$

where $v_{x,1}$ is the upstream velocity component along the shock normal and p_1 and β_1 the upstream thermal pressure and plasma beta, respectively; while γ denotes the ratio of specific heats. These conditions are derived from the Rankine-Hugoniot jump conditions in 1D MHD flows (Kennel et al (1989); Steinolfson and Hundhausen (1990)).

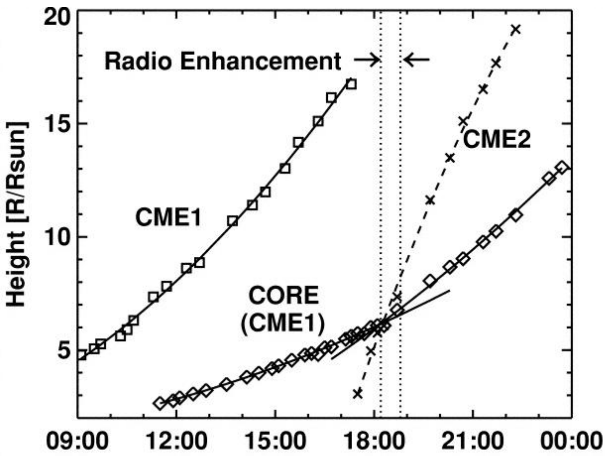

Figure 2. Height-time plot of a slow and a fast CME showing the sudden increase in the speed of the slow-CME due to the impact of the fast CME (from N. Gopalswamy et al. (2001))

3. CME PROPAGATION AND SHOCK COLLISIONS

MHD shocks accelerate particles and these accelerated particles emit radio waves. As a result, the shocks generated by CMEs *can* be observed in the corona and IP medium, e.g. by the Wind/WAVES instrument (e.g. Gopalswamy et al (2001)). The IP signals of CMEs do not always possess the typical three-part structure of most CMEs in the low corona (bright loop, dark void, bright inner kernel). As a matter of fact, a lot of questions regarding the propagation speed and the evolution of the CME structure and the geometry of the leading shock front remain to be answered.

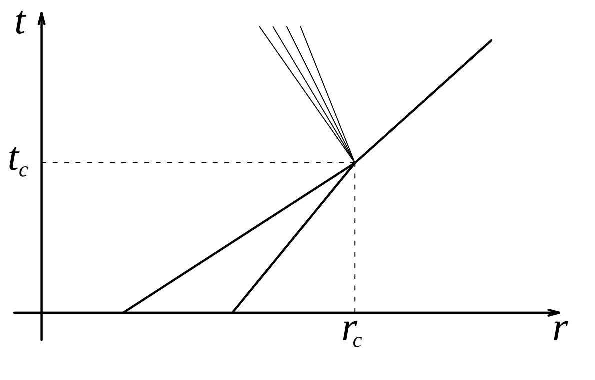

Figure 3. A collision of two shocks of the same family results into a shock of that family plus a rarefaction wave (of another family).

In addition, on the recent Shine 2001 meeting (June 2001, USA) Burlaga claimed that about one third of the interplanetary ejecta are 'magnetic clouds' while the other two thirds are 'complex ejecta'. The latter have a complicated magnetic field structure, last several days and may contain several shocks. Such events most probably consist of two or more CMEs with different speeds coming together. The well-known '2000 Bastille-day' event, e.g., produced five CMEs with their corresponding shocks overtaking each other. Hence, such interactions or 'collisions' of different IP ejecta need to be studied in order to understand the observations. Gopalswamy et al (2001) made a detailed and careful analysis of radio observations of two CMEs at different speeds originating from the same region on the Sun. These authors constructed a height-time plot of the slow and the fast CME which shows the sudden increase in the speed of the slow-CME core due to the impact of the fast CME shock (see Fig. 2). During this collision a broad-band and complex radio enhancement is observed in the radio signature from the Wind/WAVES dynamic spectrum in the 1–14 MHz range.

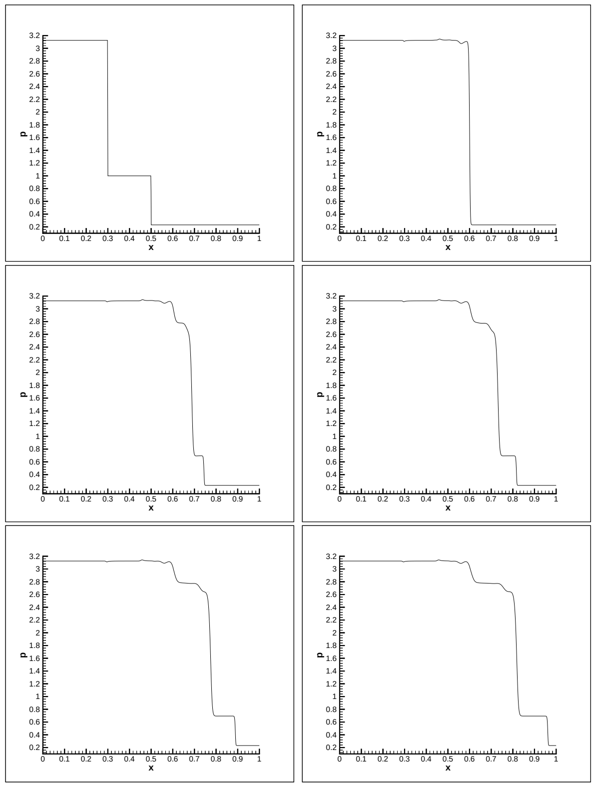

Figure 4. Results of a 2D MHD simulations. Snapshots of the pressure profile of two colliding **MHD** *shocks at* $t = 0.50, 0.60, 0.64, 0.66, 0.68,$ *and* 0.70*. The shock collision takes place at* $x = 0.6$ *and* $t = 0.6$*.*

In hydrodynamics, it is well-known that when two shocks collide the two discontinuities merge into one discontinuity that no longer satisfies the Rankine-Hugoniot condition(s). Several scenario's are possible. The observation of Gopalswamy et al (2001) seems to correspond to the case where two shocks of the same family collide, resulting in a shock in that same family. However, such a shock collision also causes a rarefaction wave of another shock family (see the illustrative sketch in Fig. 3. The resulting shock propagates in the same direction as the original shocks at an intermediate speed. The rarefaction wave, however, propagates backwards. Clearly, in MHD this picture gets more complicated due to the fact that there are now three characteristic velocities instead of just one which gives rise to a wider variety of shock families, as discussed above. Moreover, the shocks we are interested in are superposed on the solar wind.

In figures 4 and 5 six snapshots are shown of the pressure and density profiles of two colliding MHD shocks (2D simulation). The first shock is initiated at $x = 0$ and $t = 0$ and has speed $C_{s1} = 1$. At time $t = 0.4$, when the first shock is already at $x = 0.4$, a second shock is launched at $x = 0$ with speed $C_{s2} = 3$. Hence, the two shocks collide at $x = 0.6$ at time $t = 0.6$. This results in the formation of a *stronger shock*, with a strength that is almost the sum of the strengths of the two initial shocks. However, part of the energy goes into a *small expansion wave* which travels to the left(!) and also to a *contact discontinuity* traveling to the right at a smaller velocity as is clear from the two last snapshots shown in Fig. 5.

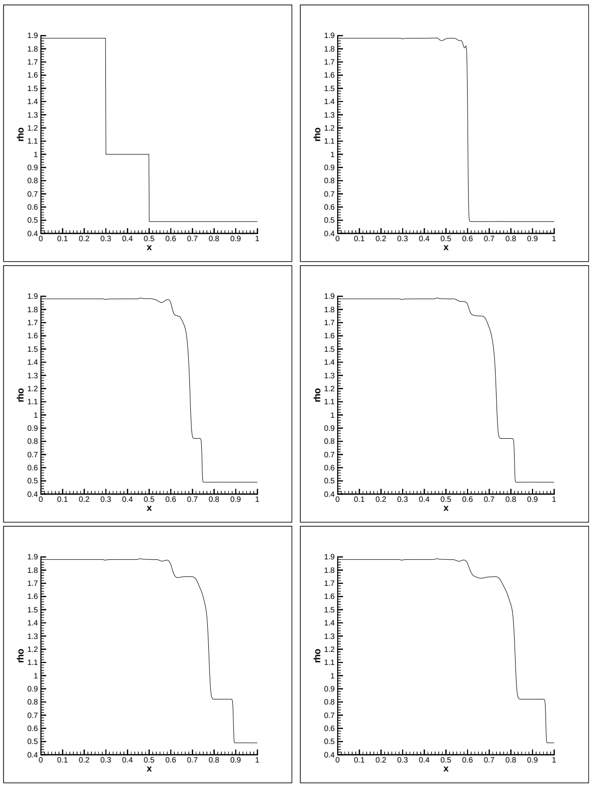

Figure 5. Snapshots of the density profile for the same shock collision as in Fig. 4.

Hence, even in this very simple setup the interaction of the two colliding MHD shocks is *non-trivial*. Since such shock interactions seem to occur frequently ('two thirds') in the IP medium, numerical simulations of such complex events may reveal some of the properties of the CMEs involved. Therefore, the simulations need to be improved: 3D geometry effects need to be taken into account, the shocks need to be superposed on the background wind, more realistic states need to be considered, etc.; and analyzed in more detail! Also, one should look after more observational signatures of such shock interactions, e.g. the rarefaction wave and the contact discontinuity, so that detailed comparisons can be made of the simulation results and the observations.

The radio signal related to the case analyzed by Gopalswamy et al (2001) (not shown here) does not show signals of a second shock nor a shock after the collision. In fact, in this case the two shocks did not collide: the radio enhancement was caused by the collision of a fast shock (of the second CME) and the core of the first (slow) CME. We looked for other interesting cases to analyze. Fig. 6 shows a good candidate for two colliding shocks. However, after the collision there is no signal of the rarefaction wave nor of the tangential discontinuity. This may be due to observational constraints (the limited dynamic range of the Wind/WAVES instrument) or due to the physics of acceleration of particles by such (weaker) shocks…

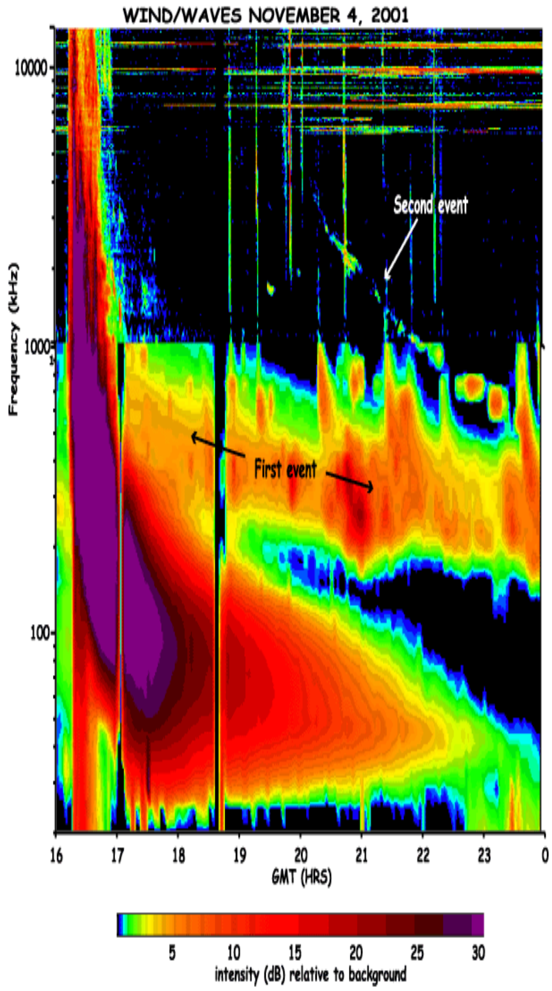

Figure 6. Wind/WAVES dynamic *spectrum in the 1-14 MHz range obtained by the RAD2 receiver, 04/11/2001.*

4. CME IMPACT: SHOCK TRANSITIONS

The strength and the structure of the bow shock at the Earth's magnetosphere depends on a lot of parameters, including $\vec{V}$, $\vec{B}$, θ_{vB}, $\vec{V}_{\rm wind}$, ... It is very likely that *during the impact of a magnetic cloud* the upstream wind becomes magnetically dominated enough to satisfy the above two 'switch-on shock' conditions ((1) and (2)). In that case, a shock front that contains a 'perpendicular' point (i.e. a point where the magnetic field is perpendicular to the shock front, see Fig. 7) can not entirely be of the [1]–[2] shock type. As a matter of fact, in Fig. 7a it is illustrated that at point B the two shock segments can not be linked to each other in a continuous way as the finite deflection of the magnetic field from the shock normal would suddenly change sign at that point.

Numerical simulations (De Sterck and Poedts (1999c)) show that a ‘magnetically dominated’ plasma flow solves this problem by creating a more complex shock topology to channel the flow around the spherical object, as sketched in Fig. 7b. The shock front segment A-B is a [1]–[2] fast shock, while B-D is of the intermediate shock type and D-E is of the fast type again. The type of the secondary shock front D-G is not clear. Finite volume simulations led to the conclusion that this is a [2]–[4] intermediate shock evolving into a [2=3]–[4] slow switch-off shock and a [3]–[4] slow shock along the shock front. But recently, the same simulations with the THOR code (based on a residual distribution discretization) revealed that this D-G shock front may entirely be of the intermediate type (Csík et al (2001); Poedts et al (2001)). The issue is not resolved yet and requires more simulations with higher spatial resolution.

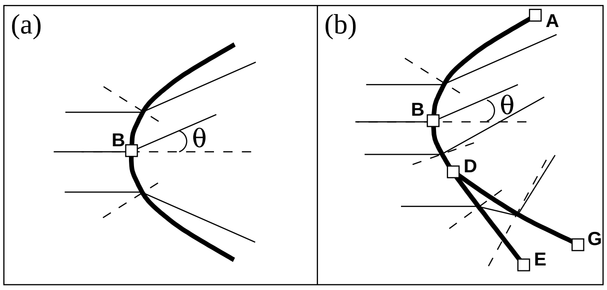

Figure 7. Topology of 3D flow over a sphere (from De Sterck et al. ’99)

As a result, the bow shock structure and the related magnetic reconnection processes are drastically affected by the impact of a magnetic cloud, especially in the parameter domain that allows fast switch-on shocks. Therefore, it is worthwhile to verify the (speculative) hypothesis that IF the condition(s) for switch-on shocks are satisfied during magnetic cloud impact, THEN the magnetic clouds have a *high geo-effectiveness*.

We included time-accurate boundary conditions in order to simulate the impact of a magnetic cloud on the Earth’s magnetospheric bow shock. The impact of the magnetic cloud is modeled by decreasing the plasma beta (i.e. increasing the magnetic field) at the inlet boundary during the impact simulation while keeping the magnetic cloud velocity and density constant. Also the angle θ_{vB} between the magnetic field lines and the stream lines at the inlet boundary is fixed at 5 degrees. Figure 8 displays the time dependent plasma β which is initially outside the switch-on domain for this parameter choice (between the two dashed lines in Fig. 8). During the cloud impact, the plasma beta transverses the switch-on regime twice coming back to its initial value from where it is kept constant again.

In Figure 9 four snapshots are shown of the density and magnetic field lines corresponding to the four positions in parameter space indicated in Fig. 8. Strikingly, the secondary shock front is present from in the beginning of the simulation which starts outside the switch-on regime.

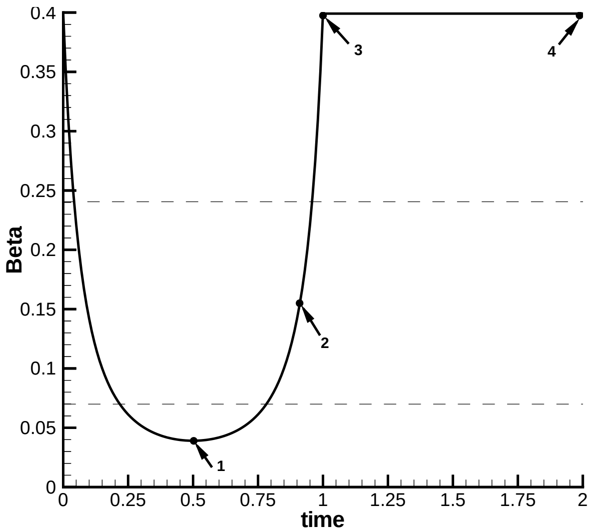

Figure 8. The profile of the time-dependent plasma β in the simulations. The parameter domain for switch-on shocks (based on the formulas (1) and (2), derived from 1D MHD is indicated by the two horizontal dashed lines.

However, as mentioned before the conditions (1) and (2) are derived in a 1D situation and probably this result can not simply be extrapolated and applied to the 3D case. This seems to indicate that in 3D the switch-on regime may be much larger.

As can be seen on Fig. 9 the shock topology changes drastically when the magnetic cloud arrives and the magnetic field lines change accordingly . As a result, the magnetic reconnection processes at the Earth’s magnetosphere, and therefore also the geo-effectiveness, will indeed be affected drastically in this case. However, at this point we can not tell to what extent the geo-effectiveness is increased (or decreased!). The answer to this important question requires more detailed parameter studies and better resolved simulations.

5. CONCLUSIONS

Space Weather physics is very complicated. *A detailed study of the MHD shocks generated by CMEs may reveal key properties of several of its sub-problems.*

MHD shocks can be much more complex than their HD counterparts. This MHD shock complexity may be advantageous for theory because *it may yield a way to distinguish between different models and it may allow to derive parameter values by comparing observations with theoretical results*. As a matter of fact, the CME related IP MHD shocks can be observed in the long-wavelength radio spectrum (in the decameter, hectometer, and kilometer domain) which enables to some extent to follow magnetic clouds throughout their propagation towards the Earth.

During their propagation through IP space, the MHD shocks induced by fast CMEs remain complex and, in addition, interact with each other. Such shock collisions

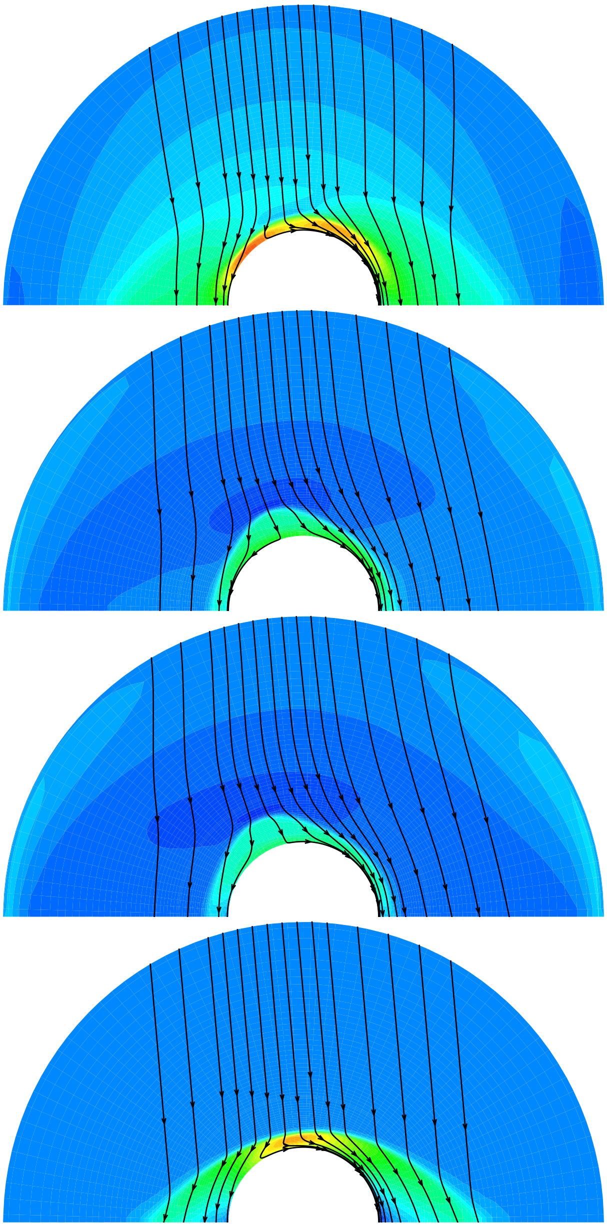

Figure 9. Snapshots of the magnetic cloud impact. Cut through the equatorial plane ($x-y$ symmetry plane cut of a full 3D simulation). Density contours (filled coloured contour lines) are superimposed by (black, solid) magnetic field lines. The snapshot times correspond to the four points indicated in Fig. 8 (point 1 corresponds to the top image, 4 to the bottom image).

have been observed and we encourage more detailed observations *and* more realistic numerical simulations. This would allow a detailed comparison of the observations and the theory. The complexity guarantees that some characteristics of the magnetic clouds and/or of the background solar wind can be derived from such comparative studies.

During the impact of a magnetic cloud, the Earth bow shock may also be in the switch-on regime, allowing complex shock structures. A 3D time-dependent MHD simulation showed that this would have a drastic effect on the evolution of the shock topology. *The secondary shocks certainly affect the geo-effectiveness of magnetic storms:* the associated switching back of the magnetic field lines must influence the reconnection process at the terrestrial magnetopause. However, much more modeling and parameter studies are required to reveal the details.

ACKNOWLEDGMENTS

These results were obtained in the framework of the projects OT/98/14 (K.U.Leuven), G.0344.98 (FWO-Vlaanderen), and 14815/00/NL/SFe(IC) (ESA Prodex 6). LVDG is supported by Research Fellowship F/01/004 of the K.U.Leuven.

REFERENCES

Antiochos S.K., DeVore C.R., and Klimchuk J.A., 1999, ApJ 510, 485–493

Chen J., 1989, ApJ 338, 453–470

Csík A., Deconinck H., and Poedts S.: 2001, *AIAA journal* 39, 1532

De Sterck H., 1999, PhD thesis, NCAR/CT 167.

De Sterck H. and Poedts S., 1999, A&A 343, 641–649

De Sterck H. and Poedts S., 1999, *in Proceedings of the 9th European Meeting on Solar Physics*, Florence, ESA-SP-448, 935–942

De Sterck H. and S. Poedts, 1999, JGR 104, 22401

Dryer M., 1982, Space Sci. Rev. 33, 233–275

Forbes T.G. and Isenberg P.A., 1991, ApJ 373, 294–307

Gopalswamy, N., S. Yashiro, M. L. Kaiser, R. A. Howard, and J.-L. Bougeret, ApJ Lett., 548, 91–94, 2001.

Kennel C.F., Blandford R.D., and Coppi B., 1989, JPP 42, 299–319

Klimchuk J.A.: Proc. of the Chapman Conference on Space Weather, AGU Monograph Series, ed. P. Song, G. Siscoe, and H. Singer, 2002, in press.

Krall J., Chen J., and Santoro R., 2000, ApJ 539, 964–982

Low B.C., 1999, in *Solar Wind Nine*, ed. by Habbal S.R., Esser R., Hollweg J.V., and Isenberg P.A., 109–114, AIP, Woodburry, NY.

Csík Á, De Sterck H., van der Holst B., Deconinck H., and Poedts S.: Proc. 15th AIAA Computational Fluid Dynamics Conference, Anaheim, California, 11–14 June 2001, *AIAA Paper 2001-2622*, 2001.

Poedts, S., De Sterck H., Van Der Holst B., Pandey B.P., Csík Á, and Deconinck H.: in *Space Plasma Simulation*, Proc. of the Sixth International School/Symposium ISSS-6, ed. J. Büchner, C.T. Dum, M. Scholer, Garching, Germany, ISDN 3-9804862-8-1, 324–327, 2001.

Steinolfson R.S. and Hundhausen A.J., 1990, JGR 95, 20693–20699

van Driel-Gesztelyi, L., Schmieder, B., and Poedts, S.: 2002, in this issue

Wu S.T., 1982, Space Sci. Rev. 32, 1150–129